

## Flexible and Scalable Multiple Access Scheme for the Broadband Mobile Satellite System

*Fumihito Yamashita<sup>†</sup>, Kiyoshi Kobayashi, Kohei Ohata, and Masazumi Ueba*

### Abstract

We investigated the design of an optimal multiple access scheme that can accommodate a wide range of applications flexibly for the next-generation mobile satellite system. After comparing several candidate schemes by computer simulation and qualitative analysis, we concluded that multirate frequency division multiple access (MR-FDMA) or orthogonal frequency division multiplexing (OFDM) is best for the forward link and that MR-FDMA is best for the return link. For MR-FDMA to accommodate a wide range of applications efficiently, the symbol rate of each user signal should be switched without quality degradation according to the user's demands or the traffic conditions. For this purpose, a new seamless symbol-rate-switchable modem has been developed. Its fundamental performances were confirmed by computer simulation.

### 1. Introduction

The next-generation mobile satellite communications systems will offer hotspot services in moving vehicles as well as content delivery, mobile phone, nomadic, and data telemetry services for people or terminals that are detached from terrestrial networks [1]-[3]. The service grade of the network will be equivalent to B3G (beyond 3G system) mobile networks. Users will access the networks through their own satellite terminals or through mobile hotspots installed on public vehicles. Mobile hotspots will enable people to access satellite networks via their own cellular terminals or personal computers (PCs), so they are the key to serving temporary users such as passengers and commuters. Nomadic services that enable broadband access anytime and anywhere, especially in mobile environments, are particularly important for video signal transmission for agencies such as news, coastguard, and disaster-relief teams. We also expect that low-data-rate telemetry services will be popular on next-generation mobile satellite

communications systems.

We estimated that the expected traffic demand throughput for mobile hotspots, nomadic services, mobile content delivery, and voice communication will exceed 1 Gbit/s in total [1]-[3]. In the envisioned system, high-speed services will be offered via portable terminals, while low-bit-rate telemetry data will be generated by ultrasmall terminals. Hence, we assume that the transmission bit rates will range from 1 kbit/s to 100 Mbit/s for the forward link and from 1 kbit/s to 20 Mbit/s for the return link.

To handle this wide range of user applications flexibly, an effective multiple access scheme is the key. Although a number of studies have compared multiple access schemes [4], [5], the results were strongly dependent on the system models used. Therefore, it was still necessary for us to find the optimal multiple access scheme for our target system. For this scheme to enable a wide range of applications, frequency/time resources should be managed flexibly, which requires dynamic frequency/time resource management.

This article focuses on designing the optimal multiple access scheme for the envisioned mobile satellite communications system and then addresses technical issues related to handling a wide range of speeds cor-

<sup>†</sup> NTT Access Network Service Systems Laboratories  
Yokosuka-shi, 239-0847 Japan  
Email: yamashita.fumihito@lab.ntt.co.jp

responding to user applications.

## 2. Optimal multiple access schemes for the next-generation mobile satellite communications system

### 2.1 Communications system

The next-generation mobile satellite communications system will offer mobile satellite communications services around the Japanese archipelago and its exclusive economic sea zone using about 70 beams [1]-[3]. Previous studies have clarified that the envisioned system, which uses multiple frequency reuse based on units of three beams, can greatly increase the total system capacity compared with the alternative of single frequency reuse [6]. The concept of multiple frequency reuse with three beams is shown in **Fig. 1(a)**. Here, the three beams share the total system bandwidth. For the purpose of multiple frequency reuse, beam coverage areas that make use of the same frequencies are geographically separated. Thus, co-frequency interference among beams is mitigated and the total system capacity exceeds that offered by single-frequency reuse.

We assume that our multibeam system will use the frequency allocation scheme shown in **Fig. 1(b)** to cope with traffic fluctuations while maximizing the total capacity. The system bandwidth is set in terms of frequency segments, and the frequency boundary scheme uses the parameter of frequency segment.

define the frequency allocation scheme as variable boundary multiple frequency (VMF) allocation [6].

### 2.2 Wide-range multiple access scheme

We have to consider a 50-dB-wide data range from 1 kbit/s to 100 Mbit/s in designing the optimal multiple access scheme. At the same time, we should take into account terminal capability. For instance, ultra-small terminals require low battery consumption, so a low clock-rate signal processor and a small high-power amplifier (HPA) are needed. Thus, in spite of their inherent rate flexibility, high-speed TDMA (time division multiple access) and wideband CDMA (code division multiple access) are not acceptable. To absorb traffic distributions, the VMF scheme should multiplex user channels on a segment-by-segment basis. This means that a multicarrier system can strike a balance between these conditions.

The multiple access scheme considered to be suitable for the envisioned system is shown in **Fig. 2**. MR-FDMA (multirate frequency division multiple access) is currently used in the Ku-band satellite communications system. Different frequency slots are assigned to each user for every call origination. MC-OCDMA (multicarrier orthogonal CDMA) discriminates users by using orthogonal codes. It is currently applied to third-generation mobile cellular communications. MC-TDMA (multicarrier TDMA) allocates each user different time and frequency slots. MC-TDMA is used for various types of satellite

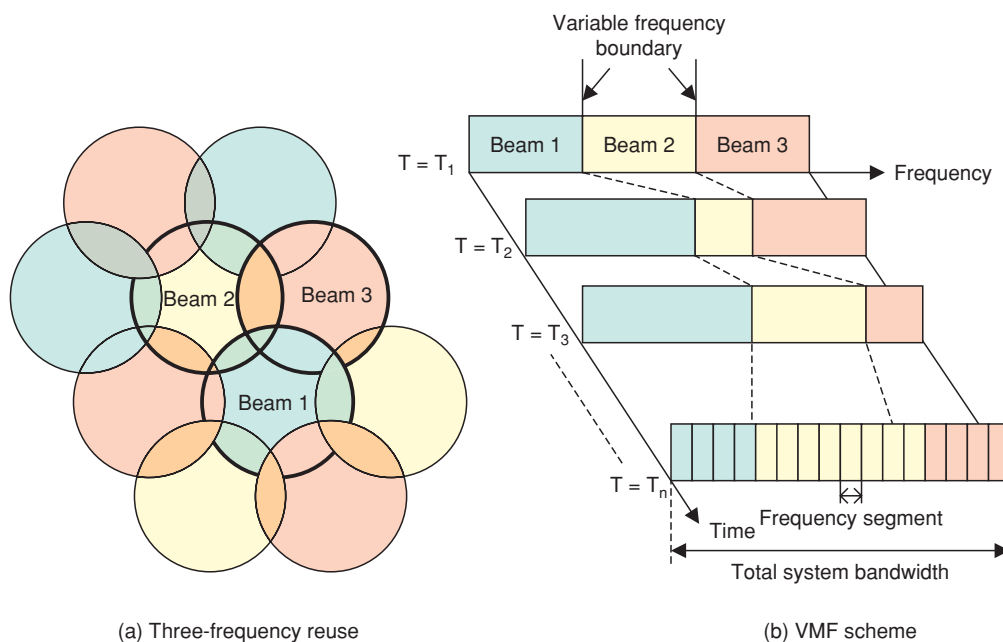


Fig. 1. Multiple frequency reuse with three beams and frequency allocations with VMF scheme.

and/or terrestrial wireless communications. OFDM (orthogonal frequency division multiplexing), which multiplexes multicarrier signals orthogonally in the frequency domain, is currently used in terrestrial wireless local area networks.

Choosing the best mobile satellite communications

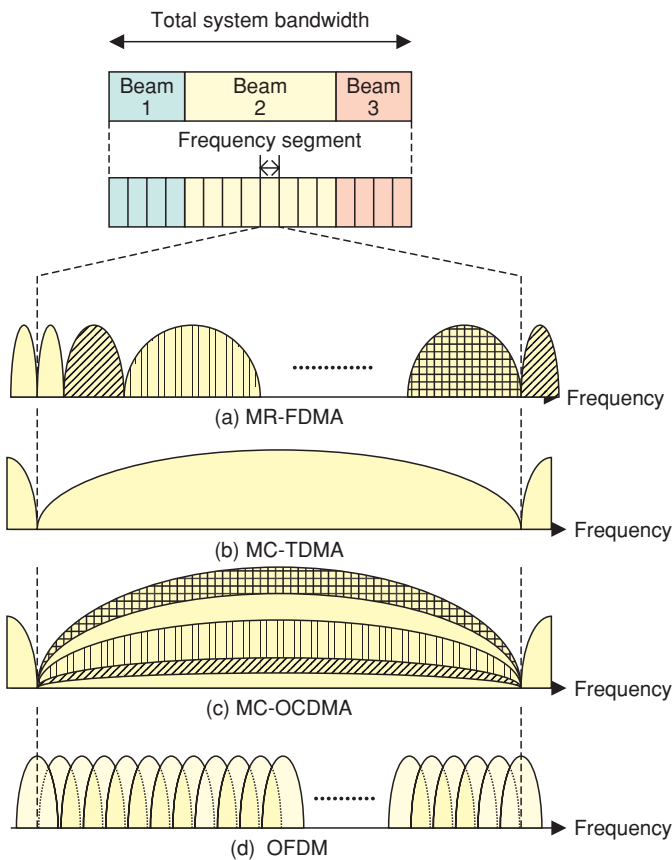


Fig. 2. Multiple access schemes.

system requires identifying the optical multiple access scheme. Therefore, we evaluated the above four candidates through quantitative performance evaluations and qualitative analyses.

### 2.3 Bit error rate evaluation of multiple access schemes

To achieve higher power utilization efficiency, a multiple access scheme within one segment should meet the required bit error rate with smaller transmission power. We evaluated the required  $E_b/N_0$  value\* considering the effect of the non-linearity of amplification and fading, both of which are specific to mobile satellite communications. The main simulation parameters are listed in **Table 1**. In the simulations, the number of channels in each segment and the baud rate of each channel were set to the same value. Thus, the occupied bandwidth of each segment is determined considering the roll-off pulse shaping (for MR-FDMA, MC-TDMA, and MC-OCDMA) or guard interval insertion (for OFDM). The occupied bandwidth of each segment was set to roughly 2 MHz, and the system bandwidth was assumed to be divided into roughly 16 segments. For coherent detection, pilot symbols are inserted periodically. Frame efficiency with pilot insertion is 0.875, regardless of the multiple access scheme. Multipath delay  $\tau$  was assumed to be less than 0.6 ms [7], a typical value in land mobile satellite communication channels. Although forward error correction was not simulated, its effect was taken into consideration by comparing required  $E_b/N_0$  values for a bit error rate (BER) of  $2 \times 10^{-2}$ . This

Table 1. Main simulation parameters.

	MR-FDMA	MC-TDMA	MC-OCDMA	OFDM
Occupied bandwidth	2.376 MHz			1.982 MHz
No. of channels	64			
Baud rate per channel	30 kbaud			
Modulation	QPSK			
Roll-off rate	0.2			
Demodulation	Pilot aided coherent detection			
Fading	Rician fading C/M = 10 dB			
Max. doppler frequency	100 Hz			
Other parameters			2 finger rake	Guard interval = 1 $\mu$ s

\*  $E_b/N_0$  means the ratio of energy per bit ( $E_b$ ) to the spectral noise density ( $N_0$ ). It is a measure of signal-to-noise ratio for a digital communication system.

value without forward error correction corresponds to a BER of  $10^{-8}$  with a typical turbo product code.

**Figure 3** shows the overall performance with non-linear amplification, OBO (output backoff) = 3 dB, and frequency selective fading channels (Rician fading C/M (ratio of carrier power to multipath power) = 10 dB). We found that MC-TDMA and MC-OCDMA showed considerable degradation when  $\tau$  was large. Due to its fast baud rate, MC-TDMA was sensitive to multipath delays and we saw delayed multipath signal interference affecting the adjacent symbol. Although MC-OCDMA used rake diversity, the degradation due to inter-code interference exceeded the diversity gain when the channel was fully loaded. Conversely, MR-FDMA and OFDM were immune to fading because their symbol period was long enough

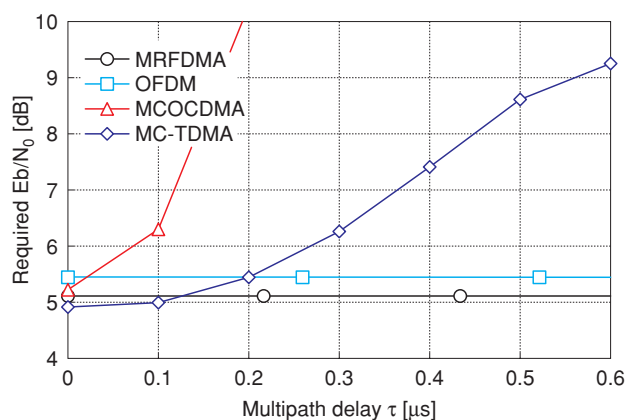


Fig. 3. Required  $E_b/N_0$  vs. multipath delay (OBO = 3dB).

compared with  $\tau$ .

## 2.4 Overall evaluation of multiple access schemes

Overall evaluation results are summarized in **Table 2**. We evaluated the important factors such as system capacity, multipath tolerance, terminal power consumption, and required transmission power control accuracy.

### 2.4.1 Forward link multiple access scheme

For the forward link, all candidates showed approximately equivalent performance except for multipath tolerance. As shown in Fig. 3, MR-FDMA and OFDM offered lower required  $E_b/N_0$  values than the others. This means that these two schemes can effectively utilize the system power resource, so they can achieve higher system capacity than the other schemes.

### 2.4.2 Return link multiple access scheme

For the return link, MR-FDMA and OFDM outperformed the others. The difference was the terminal's power consumption. Since the power consumption of the user terminal is dominated by the HPA, its power efficiency is very significant. OFDM was not feasible because it requires a high-performance HPA due to its use of multicarrier signal transmission. In MR-FDMA, since one user transmits a single carrier signal, the amplifier requirements are more relaxed. Thus, a small cost-effective HPA, suitable for battery-powered terminals, can be used. Consequently, we concluded that MR-FDMA is the best multiple access scheme for the return link of the envisioned system.

Table 2. Comparison of multiple access schemes.

Subject		MR-FDMA	MC-TDMA	MC-OCDMA	OFDM		
					Time	Frequency	
Transmission Capacity	FWD	0.1–10% loss <sup>a</sup>			0.1–10% loss <sup>b</sup>		
	RTN	0.1–10% loss <sup>a</sup>	0.1–10% loss <sup>c</sup>	50% loss <sup>d</sup>	0.1–10% loss <sup>c</sup>	50% loss <sup>e</sup>	
Multipath tolerance		No degradation (< 500 kbaud)	Severe degrade (delay > 1/2 symbol)	Severe degrade (code usage > 50%)	No degradation (GI > 1 $\mu$ s)		
Terminal power consumption		Small (low OBO)	Large (burst transmission)	Large (high OBO)			
TPC accuracy	FWD	Low	Low	Low	Low		
	RTN			High			
Rating	FWD	Low bit/s	Excellent	Fair	Fair	Good	
		High bit/s	Good	Poor	Fair	Excellent	
	RTN	Low bit/s	Excellent	Fair	Poor	Fair	Poor
		High bit/s	Good	Poor	Poor	Fair	Poor

<sup>a</sup>Guard band loss

<sup>b</sup>Guard interval (GI) loss

<sup>c</sup>Guard band + guard time

<sup>d</sup>Inter-code interference

<sup>e</sup>Inter-symbol interference

### 3. Seamless symbol rate switching technique for highly scalable MR-FDMA

#### 3.1 Variable communication speeds

As described in the previous section, the VMF scheme can provide scalable frequency resource management by changing the number of segments assigned to each beam. In the VMF scheme, a wide range of applications will be mixed in one frequency segment. Thus, depending on the user traffic and applications in use, assignable frequency/time resources could fluctuate drastically. To improve the frequency utilization efficiency while satisfying user demands flexibly, we need frequency/time resource reallocation.

Based on the discussion in Sec. 2, we concluded that MR-FDMA and OFDM are the most promising multiple access schemes for the next-generation mobile satellite communications system. The concept of flexible frequency/time resource allocation for MR-FDMA and OFDM is introduced in Fig. 4. Many users will share each frequency segment. In MR-FDMA (Fig. 4(a)), when several users (B, C, and E) disconnect communications at  $T = T_2$ , the vacant frequency band is reassigned to user D, who has requested a higher communication speed. In OFDM, all users share the whole frequency segment and available time slots are allocated to each user according to the requests made. As shown in Fig. 4(b), OFDM can support variable communication speeds by adjusting the number of time slots assigned.

frequency segment and demodulates it all the time. Thus, no discontinuity will occur when individual communication speeds are changed.

On the other hand, in MR-FDMA, variable communication speeds are achieved only by switching the user's symbol rate, as shown for user D in Fig. 4(a). However, since symbol rate switching entails switching the symbol clock rate, it causes a loss of synchronization, which degrades signal quality. Such synchronization loss is a technical issue that must be overcome if dynamic frequency resource management is to be successful. Therefore, we focused on a new symbol rate switching technique for MR-FDMA access that does not harm the communication quality.

#### 3.2 Seamless symbol rate switching technique for MR-FDMA modem

To switch the user's symbol rate without degrading communication quality, we developed a seamless symbol rate switching technique for the MR-FDMA modem. Its overall configuration is shown in Fig. 5. To avoid synchronization loss when changing symbol rates, this modem newly implements a clock phase compensator [9]. The signal processing flow of this modem is as follows. In the transmitter (Tx), signals are modulated by the clock from the synchronous clock generator. Its clock speed is denoted as  $M \times R$ , where  $R$  is the symbol rate and  $M$  is the oversampling ratio. Next, the sampling rate is converted to  $f_{\text{samp}}$  by the resampler, where  $f_{\text{samp}}$  is the Tx sampling rate fed from the Tx system clock oscillator. To implement this action, the resampler interpolates the input sig-

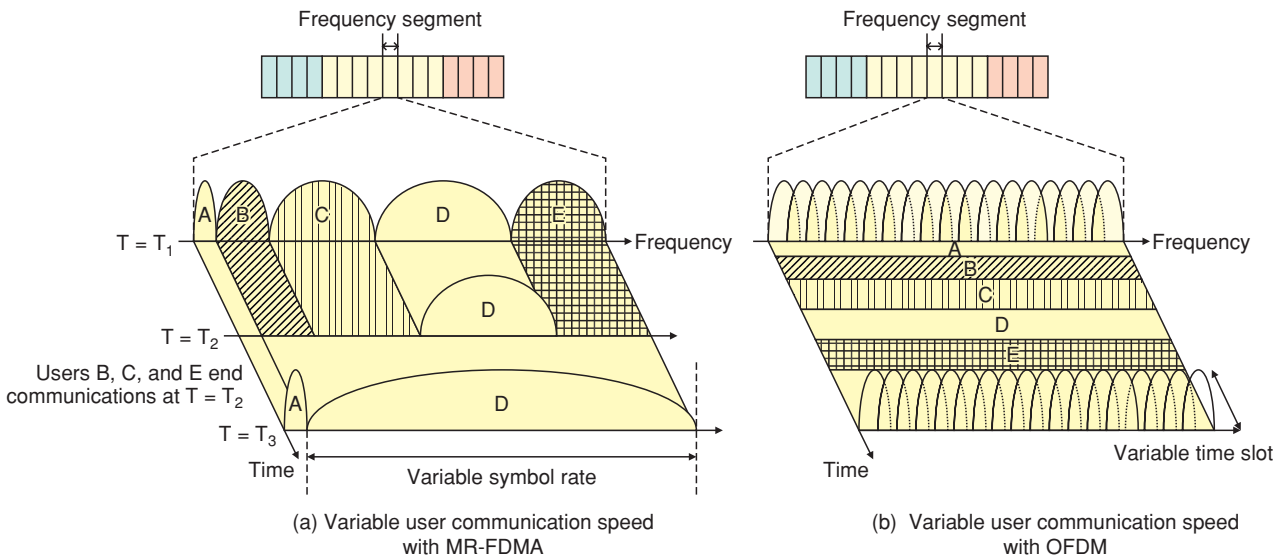


Fig. 4. Variable user communication speed in one frequency segment.

nals. In the receiver (Rx), the sampling rate is converted by the resampler from  $f_{\text{samp}}$  to  $MR$ , where  $f_{\text{samp}}$  is the Rx sampling rate fed from the Rx system clock oscillator.

The clock timings used in Fig. 5 are shown in Fig. 6. In Fig. 6(a), the clock from the system clock oscillator is defined as the system clock. The positive edge of the system clock is defined as the system timing. As shown in Fig. 6(b), the Nyquist clock is defined as  $M$  times the Nyquist sampling clock, which is asynchronous to the system timing. Since the Nyquist sampling clock rate is equal to symbol rate  $R$ , the rate of the Nyquist clock is denoted as  $MR$ . In Fig. 6(b), the positive edge of the Nyquist clock is defined as the symbol timing. To link the Nyquist clock to the system timing, the clock phase and synchronous clock are introduced, as shown in Figs. 6(c) and (d). The clock phase is the phase of the Nyquist clock while the synchronous clock is the clock pulse located at the system timing just after symbol timing. Modulation and demodulation are performed with the synchronous clock. In this variable symbol rate modem, the symbol rate is switched by changing the synchronous clock according to the symbol rate.

Symbol rate switching is carried out after Tx and Rx symbol timings have been initially synchronized by the Rx timing recovery circuit. The Tx and Rx clock relationship before symbol rate switching is shown in Fig. 7. As shown in Figs. 7(a) and (b), the Tx and Rx symbol timings are synchronized to each other in this state. This means that the Tx and Rx clock phases are also synchronized. The symbol rate is switched at the boundary of the signal frames. This frame boundary is defined on the symbol timing between signal frames. Thus, to switch symbol rates, this frame boundary and the new symbol rate information must be shared between Tx and Rx in advance through the control channel. Based on this information, Tx and Rx switch the symbol rate at the dedicated frame boundary.

The relationship of Tx/Rx clock phases around the dedicated frame boundary at which symbol rate switching is performed is shown in Fig. 8. As shown by (a), symbol rate switching entails a clock phase error when the conventional technique is used. This is because Tx and Rx carry out symbol rate switching asynchronously. This clock phase error event causes burst errors in the demodulated signals. In the worst case, this burst error might lead to synchronization failure. However, our modem can prevent this clock phase error. The operating principle is as follows. The ratio of  $R_2/R_1$ , where  $R_1$  is the prior symbol rate and  $R_2$

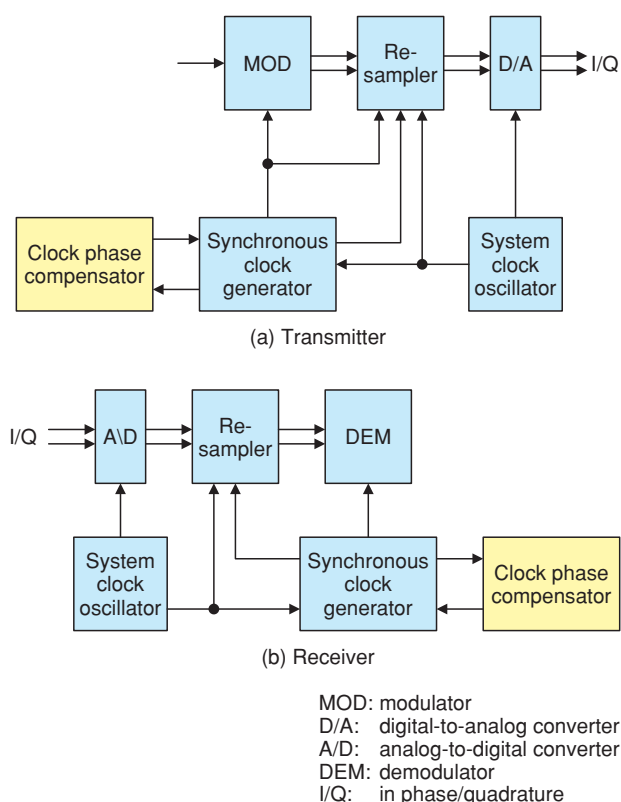


Fig. 5. Configuration of the proposed variable symbol rate modem.

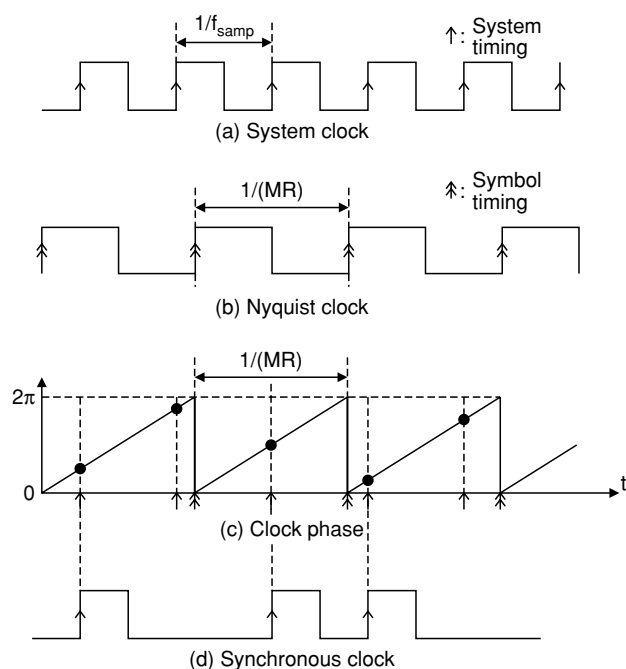


Fig. 6. Clock timing relationship in the variable symbol rate modem.

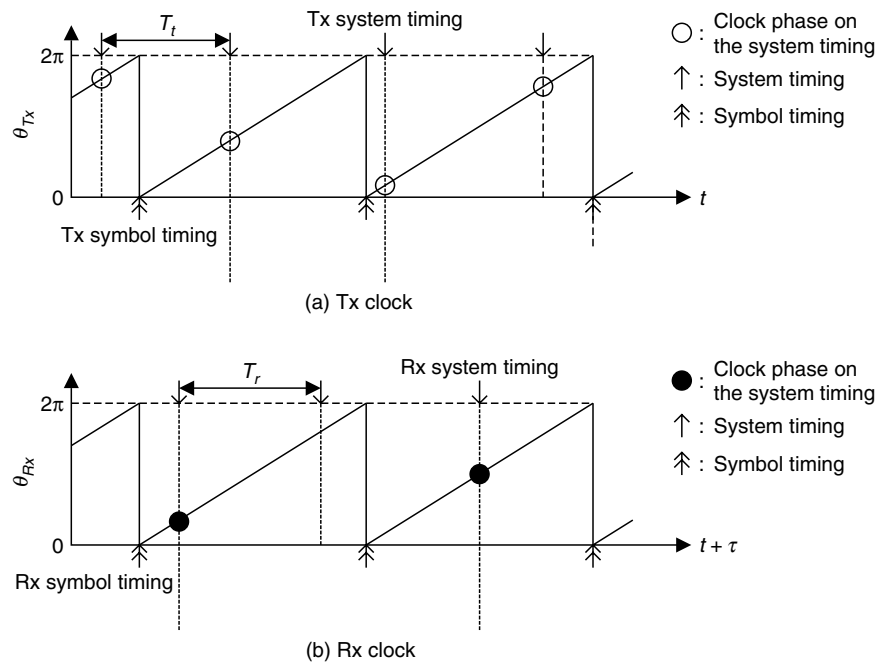


Fig. 7. Clock relationships after having achieved symbol timing synchronization.

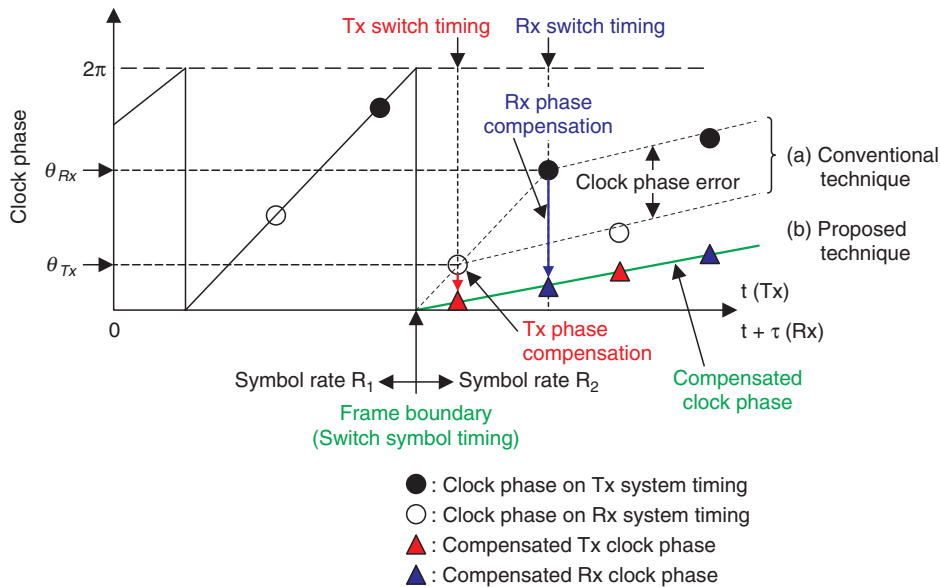


Fig. 8. Proposed clock phase compensation scheme.

is the posterior symbol rate, is multiplied by the Tx/Rx clock phase just on the Tx/Rx symbol rate switch timing. Due to this instantaneous modification of clock phase, Tx/Rx clock phases are compensated as shown by (b) so that they agree with each other. Since the Tx and Rx clock phases are the same, synchronization is maintained even after symbol rate switching. In other

words, this scheme compensates for the Tx and Rx clock phases as if the symbol rate was switched synchronously at the frame boundary. Accordingly, clock phase error caused by symbol rate switching is eliminated in this modem, so this clock phase compensation scheme enables symbol rates to be switched without degrading the communication quality.

### 3.3 Computer simulation of the symbol rate switching scheme

#### 3.3.1 Simulation conditions

We evaluated the clock phase error at the demodulator to verify our symbol rate switching scheme. The simulation conditions are listed in **Table 3**. Simulations were conducted by changing the switch timing, and their ensemble average was plotted. Symbol rate switching was carried out at the 240th symbol in all simulations.

#### 3.3.2 Performance evaluation via clock phase error

To validate the scheme's operation, we evaluated the clock phase error. We selected symbol rates arbitrarily in the range listed in Table 3. **Figures 9** and **10** show the ensemble average of the clock phase error when the symbol rate was switched from 5.3 to 10.1 MHz and from 10.1 to 1.1 MHz, respectively. In this simulation, we followed the recommendation [10] that the required clock phase error should be under 0.06 radians if the allowable BER degradation due to the clock phase error is not to exceed 0.1 dB at  $\text{BER} = 10^{-2}$ .

As shown by cases (b) and (d) in Fig. 9, the conventional modem allowed the clock phase error to exceed 0.3 radians when the symbol rate was switched. Although the disturbed clock phase eventually converged as a result of the timing recovery circuit, it still failed to meet the requirement for 4000 symbols after the symbol rate switching in case (d). On the other hand, in our modem, as shown by (a) and (c) in Fig. 9, the clock phase error was not disturbed at all by symbol rate switching and the clock phase error requirement continued to be satisfied. These results confirm that our scheme prevents an increase in clock phase error when the symbol rate is changed.

A wider range of symbol rate switching is shown in Fig. 10. The symbol rate was changed from 10.1 to 1.1 MHz. As shown in cases (a) and (c), our scheme could change the symbol rate smoothly without any increase in clock phase error. Since no unexpected clock phase error occurred at the time of symbol rate switching, we concluded that our modem switched the symbol rate while preventing all significant clock phase error. The conventional modem, on the other hand, allowed the clock phase error to exceed 0.6 radians, as shown in cases (b) and (d) in Fig. 10. While the timing recovery circuit will eventually force the clock phase error to converge, this error will be excessive until convergence is complete.

The above simulation results show that our scheme suppresses the clock phase error even when the symbol rate is changed over a wide range. Thus, the envi-

Table 3. Simulation parameters.

Modulation	QPSK
Symbol rate (R)	10.1 MHz, 5.3 MHz, 1.1 MHz
System clock oscillator	25 MHz
$C/N_0$	76 dBHz

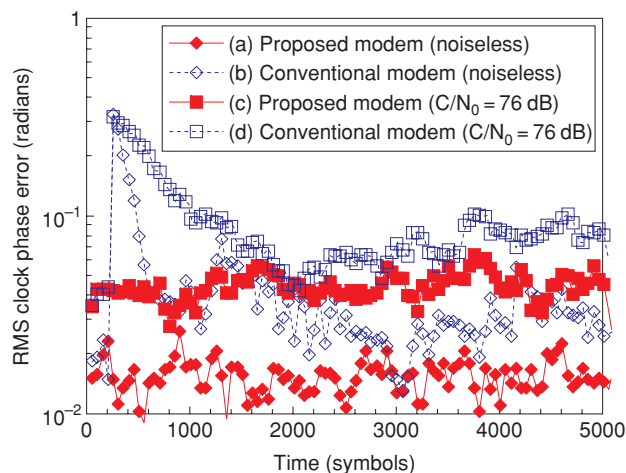


Fig. 9. Clock phase error ( $R = 5.3 \text{ MHz} \rightarrow 10.1 \text{ MHz}$ ).

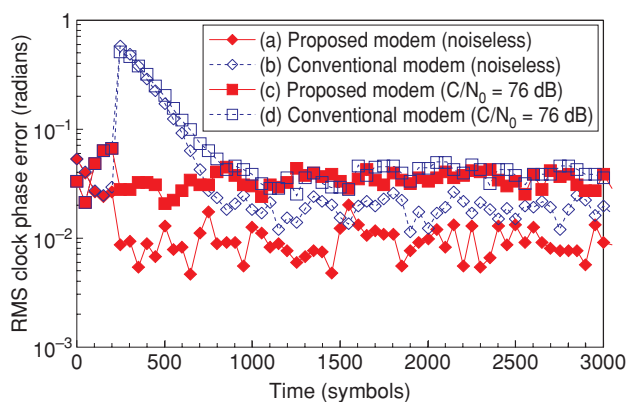


Fig. 10. Clock phase error ( $R = 10.1 \text{ MHz} \rightarrow 1.1 \text{ MHz}$ ).

sioned system enables each user using MR-FDMA to utilize the frequency bandwidth flexibly according to his/her demands or the traffic conditions.

## 4. Conclusion

We investigated an optimal multiple access scheme for flexibly and efficiently handling the various types of user applications that the next-generation mobile satellite communications system will accommodate. After comparing promising multiple access schemes by computer simulation and qualitative analysis, we concluded that MR-FDMA or OFDM is best for the



forward link multiple access scheme and that MR-FDMA is suitable for the return link.

The key to the envisioned system's ability to support a wide range of applications is whether a user can change his or her communication speed adaptively according to the traffic conditions. OFDM can support variable communication speeds simply by adjusting the number of time slots assigned among users. On the other hand, MR-FDMA requires that the users switch their symbol rates dynamically to support variable communication speeds. Simulations showed the significant problems of conventional MR-FDMA modems: they suffer from severe drops in communication quality when the symbol rate is switched due to a sudden rise in clock phase error. To overcome this problem, we developed a new seamless symbol rate switching technique. It eliminates the clock phase rise that would otherwise cause severe drops in communication quality. Simulation results showed that this scheme could change the symbol rate with no BER degradation.

We have found the optimal multiple access scheme for the next-generation mobile satellite communications system and developed a technique that allows it to handle a wide range of applications flexibly. This will greatly contribute to the establishment of an attractive next-generation mobile satellite communications system.

## References

- [1] M. Ueba, K. Ohata, J. Mitsugi, and M. Umehira, "Broadband and scalable mobile satellite communication system for future access network," 22nd ICSSC AIAA-3154, May 2004.
- [2] K. Kobayashi, K. Ohata, M. Ueba, and Y. Sagawa, "Forward Link Multiple Access Scheme for Broadband and Scalable Mobile Satellite Communication System," IEEE Vol. 6, pp. 3997-4001, Sept. 2004.
- [3] K. Ohata, K. Kobayashi, K. Nakahira, and M. Ueba, "Broad and scalable mobile satellite communication system for future access networks," Acta Astronautica Vol. 57, pp. 239-249, Sept. 2005.
- [4] Y. Sagawa, K. Ohata, and M. Ueba, "A satellite resource allocation for multi-beam satellite communication system," IEICE Tech. Report, SAT2003-125, Oct. 2003.
- [5] J. Mitsugi, Y. Nakasuga, Y. Imaizumi, Y. Suzuki, and M. Ueba, "Satellite onboard technologies for next-generation mobile satellite communication systems," IEICE Tech. Report, SAT2003-113, Oct. 2003.
- [6] K. Nakahira, K. Kobayashi, and M. Ueba, "Communication Capacity and Quality Enhancement Using a Two-Layered Adaptive Resource Allocation Scheme for Multi-Beam Mobile Satellite Communication Systems," IEICE Trans Commun, Vol. E89-A, No. 7, pp. 1930-1939, July 2006.
- [7] Y. Arakaki, T. Ikegami, H. Wakana, and R. Suzuki, "Multipath measurement in land mobile satellite communication channels," IEICE Trans. Commun, Vol. J81-B-II, No. 5, pp. 391-398, May 1998 (in Japanese).
- [8] S. Otani, Y. Tanimoto, M. Iwasaki, F. Makita, H. Kobayashi, K. Eguchi, and M. Matsuda, "Development of variable-rate digital modem for digital satellite communications systems," IEEE Globecom, pp. 148-152, Feb. 1988.

- [9] F. Yamashita, K. Kobayashi, K. Ohata, and M. Ueba, "Seamless Symbol Rate Switching Scheme for Multi-Rate FDMA Modem," IEICE Trans Commun, Vol. E89-B, No. 2, pp. 545-555, Feb. 2006.
- [10] H. Meyr and M. Moenelaey, "Digital Communication Receivers Synchronization, Channel Estimation and Signal Processing," John Wiley & Sons, U.S.A., 1998.



**Fumihiro Yamashita**

Research Engineer, NTT Access Network Service Systems Laboratories.

He received the B.E., M.E., and Ph.D. degrees in electrical engineering from Kyoto University, Kyoto, in 1996, 1998, and 2006, respectively. He joined NTT Radio Communication Systems Laboratories in 1998. He is currently working on modulation and demodulation schemes for the next-generation mobile satellite communications systems. He is a member of the Institute of Electronics, Information and Communication Engineers (IEICE) of Japan and the American Institute of Aeronautics and Astronautics (AIAA). He received the Excellent Paper Award of the 14th IEEE PIMRC in 2003 and the Young Researchers' Award from IEICE in 2004.



**Kiyoshi Kobayashi**

Senior Research Engineer, Supervisor, Satellite Communication Systems Group, Wireless Access Systems Project, NTT Access Network Service Systems Laboratories.

He received the B.E., M.E., and Ph.D. degrees in electrical engineering from Tokyo University of Science, Tokyo, in 1987, 1989, and 2004, respectively. He joined NTT Radio Communication Systems Laboratories in 1989. Since then, he has been engaged in R&D of digital signal processing algorithms and their implementation techniques including modulation/demodulation, synchronization control, and diversity for satellite and personal wireless communication systems. He is currently working on future mobile satellite communication systems. He is a member of IEEE and IEICE.



**Kohei Ohata**

Senior Research Engineer, Supervisor, NTT Access Network Service Systems Laboratories.

He received the B.E. and M.E. degrees in mechanical engineering from Keio University, Kanagawa, in 1981 and 1983, respectively. Since joining Nippon Telegraph and Telephone Public Corporation (now NTT) in 1983, he has been engaged in R&D of satellite onboard antennas, earth station systems, and satellite Internet systems. He is currently researching next-generation mobile satellite communication systems. He is a member of IEICE.



**Masazumi Ueba**

Senior Research Engineer, Supervisor, Group Leader, Satellite Communication Systems Group, Wireless Access Systems Project, NTT Access Network Service Systems Laboratories.

He received the B.E. and M.S. degrees in aeronautical engineering and the Dr.Eng. degree for work on the design methodology of highly accurate antenna pointing system from the University of Tokyo, Tokyo, in 1982, 1984, and 1996, respectively. He joined the Yokosuka Electrical Communication Laboratories of Nippon Telegraph and Telephone Public Corporation (now NTT) in 1984. He has been engaged in research on the dynamics of antenna pointing control systems of satellites and shape control systems for large antenna reflectors. He is currently researching technologies for next-generation mobile satellite communication systems. He is a member of IEICE, the Japan Society for Aeronautical and Space Sciences, and AIAA.